

Copy No. _____

FACILITY FORM 602

N66-18184

(ACCESSION NUMBER)

(THRU)

29
(PAGES)

1
(CODE)

CR-65236
(NASA CR OR TMX OR AD NUMBER)

30
(CATEGORY)



LIBRARY COPY

MAR 4 1966

**MANNED SPACECRAFT CENTER
HOUSTON, TEXAS**

GPO PRICE \$ _____

CFSTI PRICE(S) \$ _____

Hard copy (HC) 2.00

Microfiche (MF) .50

ff 653 July 65



THE *Bendix* CORPORATION

BENDIX SYSTEMS DIVISION - ANN ARBOR MICHIGAN

STUDY OF MINERAL STABILITY
IN THE
LUNAR ENVIRONMENT

BSR 1175

August 1965

Third Quarterly Progress Report

BSD Project No. 82911

Contract No. NAS 9-3734

for

NASA Manned Spacecraft Center
General Research Procurement Branch
2101 Webster - Seabrook Road
Houston, Texas 77058

BENDIX SYSTEMS DIVISION
OF
THE BENDIX CORPORATION
Ann Arbor, Michigan 48107

ILLUSTRATIONS

<u>Figure</u>	<u>Title</u>	<u>Page</u>
2-1	Infrared Spectrogram of NH_4 Feldspar made from the Madagascar Fe-Orthoclase	2-2
2-2	X-Ray Diffraction Peaks of NH_4 Feldspar made from the Madagascar Fe-Orthoclase	2-3
3-1	Antigorite - Mag-2x	3-3
3-2	Ca-Montmorillonite	3-3
3-3	Calcite - Mag-2x	3-3
3-4	Goethite - Mag-2x	3-4
3-5	Hematite - Mag-2x	3-4
3-6	Muscovite - Mag-2x	3-4
3-7	Selenite - Mag-2x	3-5
3-8	Talc - Mag-2x	3-5
4-1	Heater Filament and Thermocouple Connections with Burned Out X-Ray Sample Holder	4-2
4-2	Large Vacuum Chamber with Control Units for Testing Chemical Samples	4-4
4-3	Control Units for Cross-Chamber in The University of Michigan Department of Geology and Mineralogy	4-5
4-4	Sample Holder with Fourteen Erlenmeyer Flasks Inside Large Vacuum Chamber	4-6
5-1	Environmental Laboratories - Extreme High Vacuum Chamber	5-3

TABLES

<u>Table</u>	<u>Title</u>	<u>Page</u>
3-1	D-Values of Powder Specimens, $\overset{\circ}{A}$	3-4

SECTION 1

INTRODUCTION

This is the third quarterly report on Project NAS 9-3734, "Study of Mineral Stability in the Lunar Environment." The project was initiated on 16 November 1964; this report covers the period from 16 May 1965 to 16 August 1965.

The work has closely followed the program outlined in Bendix Systems Division's Technical Proposal BSD 965, August 1964, as supplemented by Bendix Letter 64-520-13919, 30 September 1964. Efforts during the three-month period covered in this report have been devoted to:

1. Completion of synthesis of 1 gm of ultra pure and 72 gm of standard ammonium feldspar
2. Fabrication of sample holder for storage of chemical specimens, i. e. , test minerals that will be subjected to chemical analysis at the end of the long-term experiment
3. Initiation of long-term experiment.

SECTION 2

TEST MINERALS

2.1 SYNTHESIS OF AMMONIUM FELDSPAR

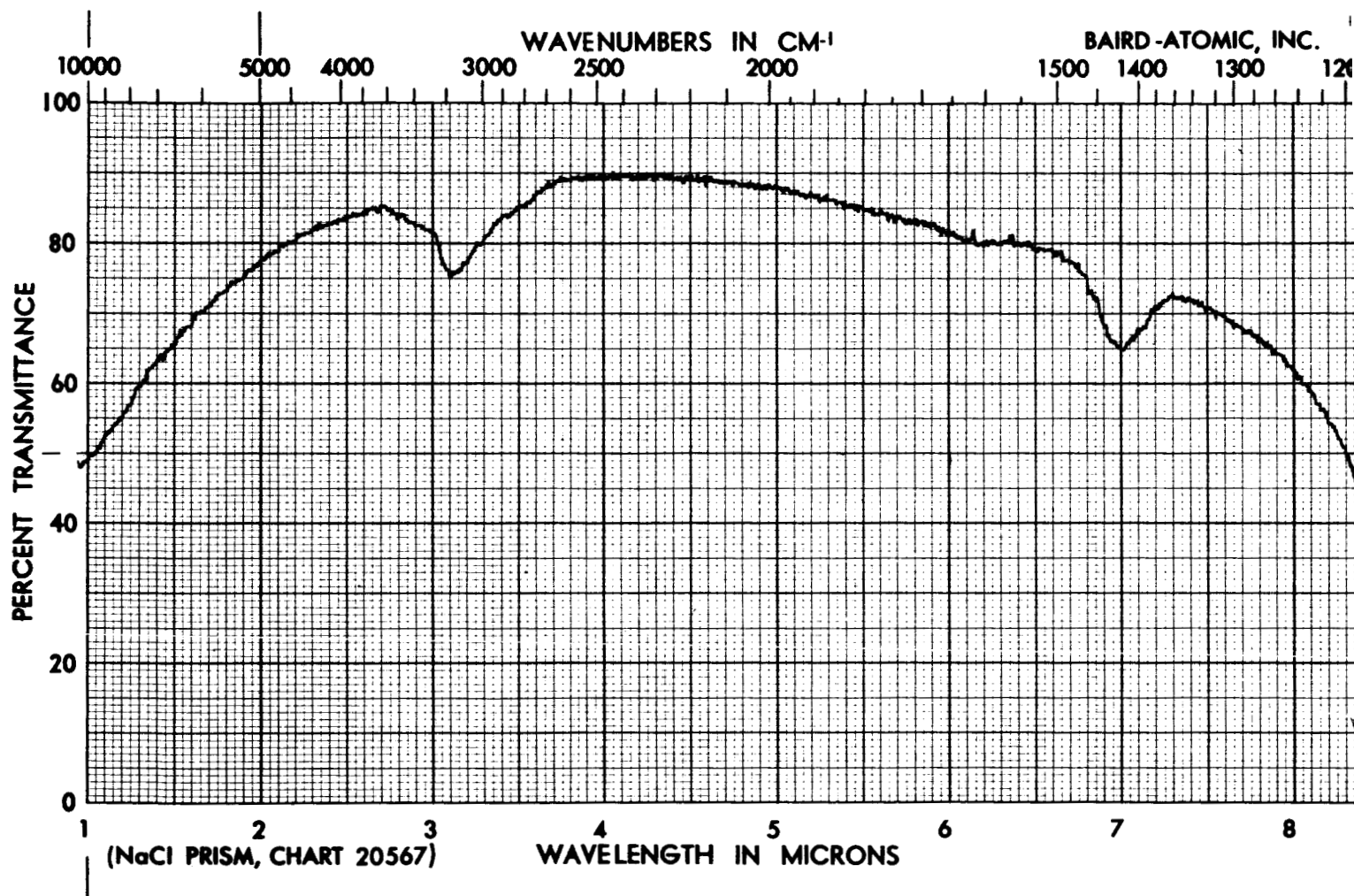
Immediately following the discussions on June 17, 1965, in Houston, work was started on producing a small amount of high purity ammoniated feldspar. This necessitated first reconditioning the seals and replacing the seal ring on the 100 ml reactor. The reactor was damaged in previous tests and had not yet been repaired.

We used the highest purity feldspar available to us as starting material, which was 2.5 gm of gemmy ferriferous orthoclase from Madagascar. This was ground to pass through a 300-mesh nylon screen and placed into thin walled gold tubes. Before sealing the tubes, a total volume of 1.35 ml of NH_4Cl solution was added. The NH_4Cl solution was made up from 4.0 ml H_2O , 1.8 gm NH_4Cl , and enough concentrated NH_4OH to bring the pH to 9.

The sealed gold tubes were then placed into the 100 ml reactor, enough water added to equalize the pressure outside the tubes with that inside, and heated to 475°C . The pressure was 9900 psi throughout the reaction period extending from July 2 to July 9. After opening the tubes, the feldspar was studied to assure that it had become ammoniated. The absorption peaks of the infrared spectrogram and the X-ray diffraction peaks both verify that this was the case. Figures 2-1 and 2-2 show these peaks.

The analysis of the high purity ammoniated feldspar presents a special problem because of the small amount produced. Consequently, it was decided that the sample should be analyzed for adsorbed water by heating to just over 100°C , then for zeolitic water by heating to just above the corresponding DTA peak, and finally for NH_4OH by heating to above the temperature of complete breakdown. Very careful weighings will be performed after each heating. Previous DTA and static weight loss studies of ammonium feldspar indicated that this procedure should give an accurate determination of the ammonium content. The remainder of the analysis will be approximated from the estimated (the iron content is uncertain) initial composition of the ferriferous orthoclase.

BAIRD-ATOMIC, INC.



1.

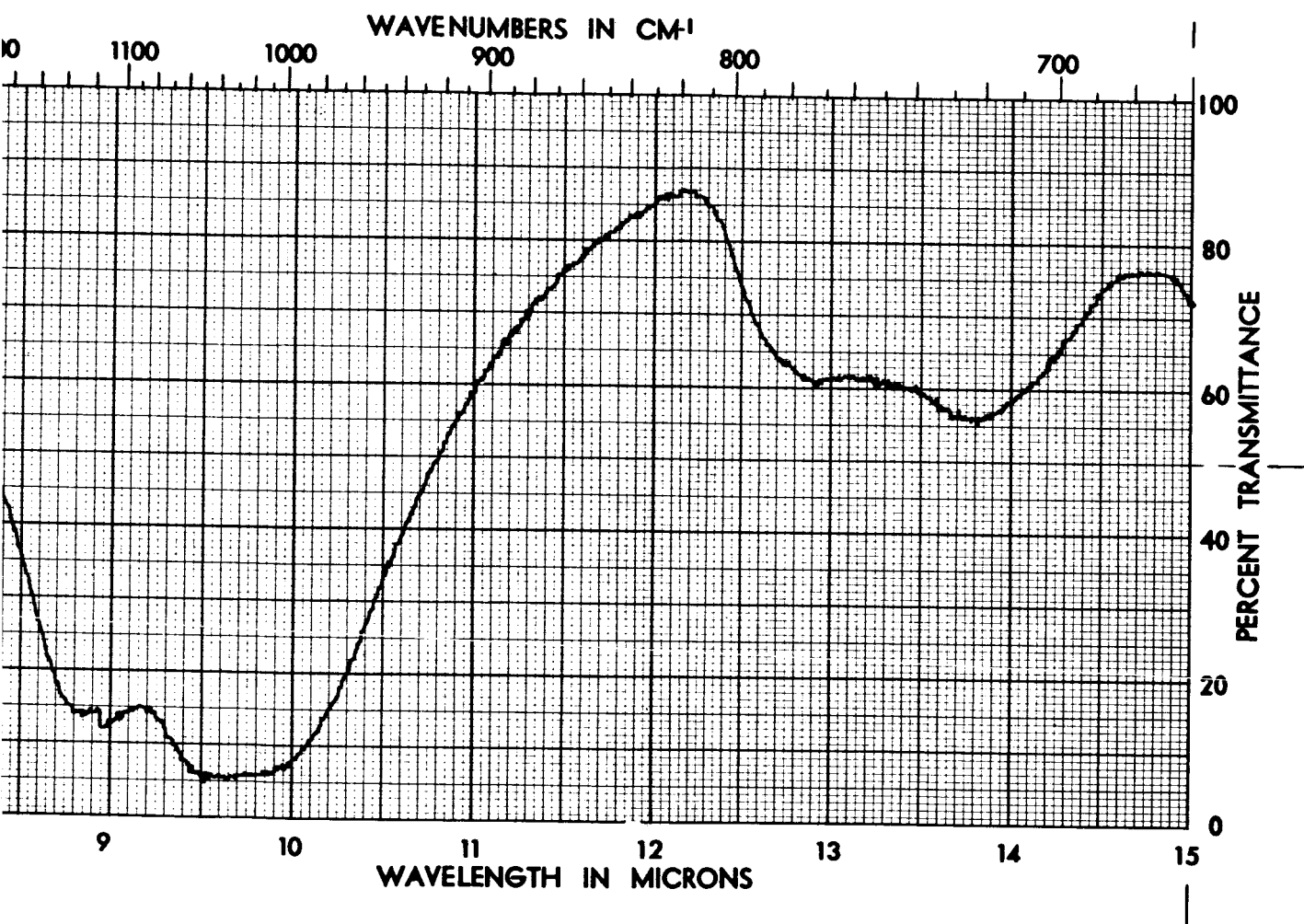
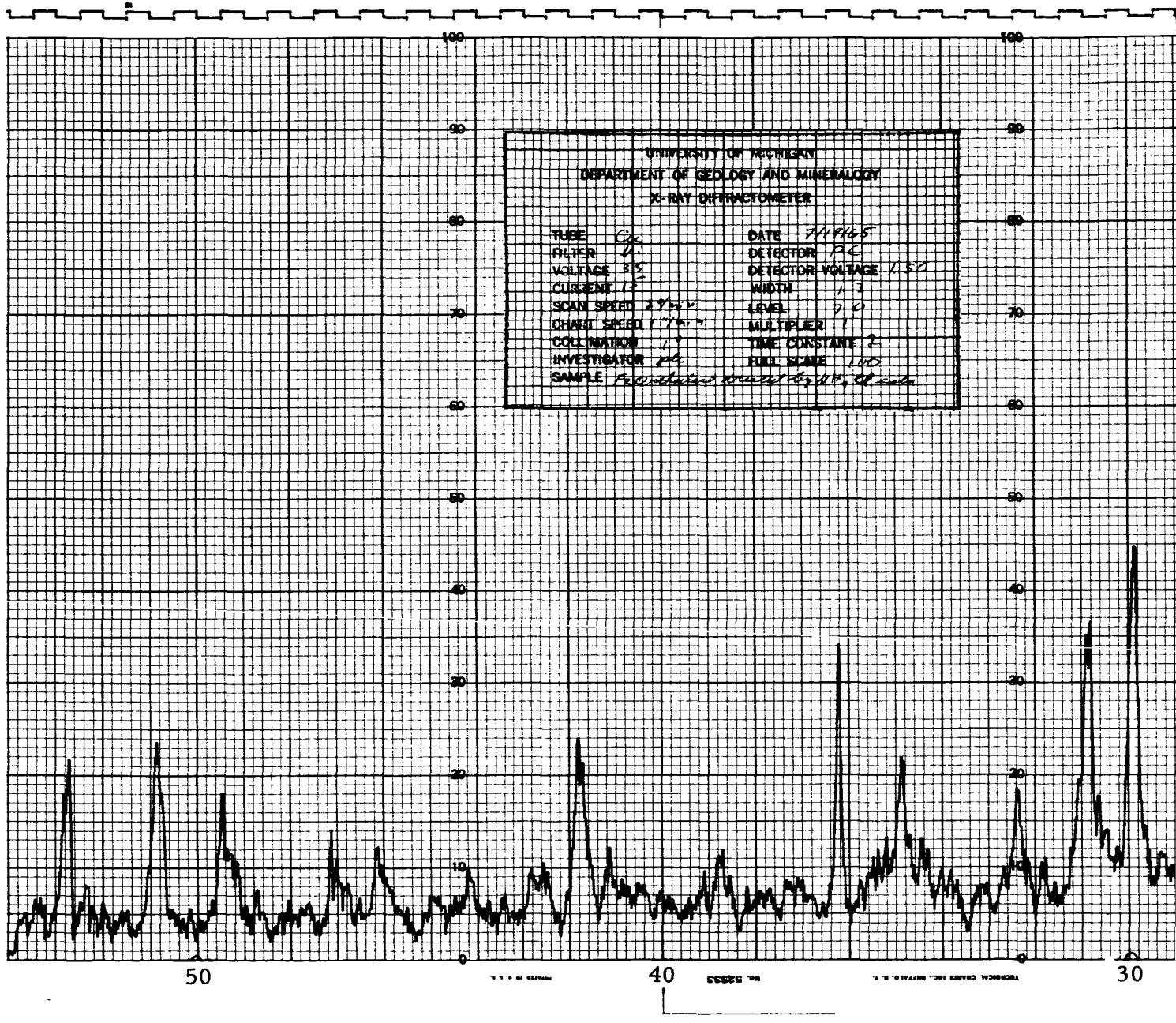


Figure 2-1 Infrared Spectrogram of the NH_4 Feldspar Made From the Madagascar Fe-Orthoclase

2.



2.

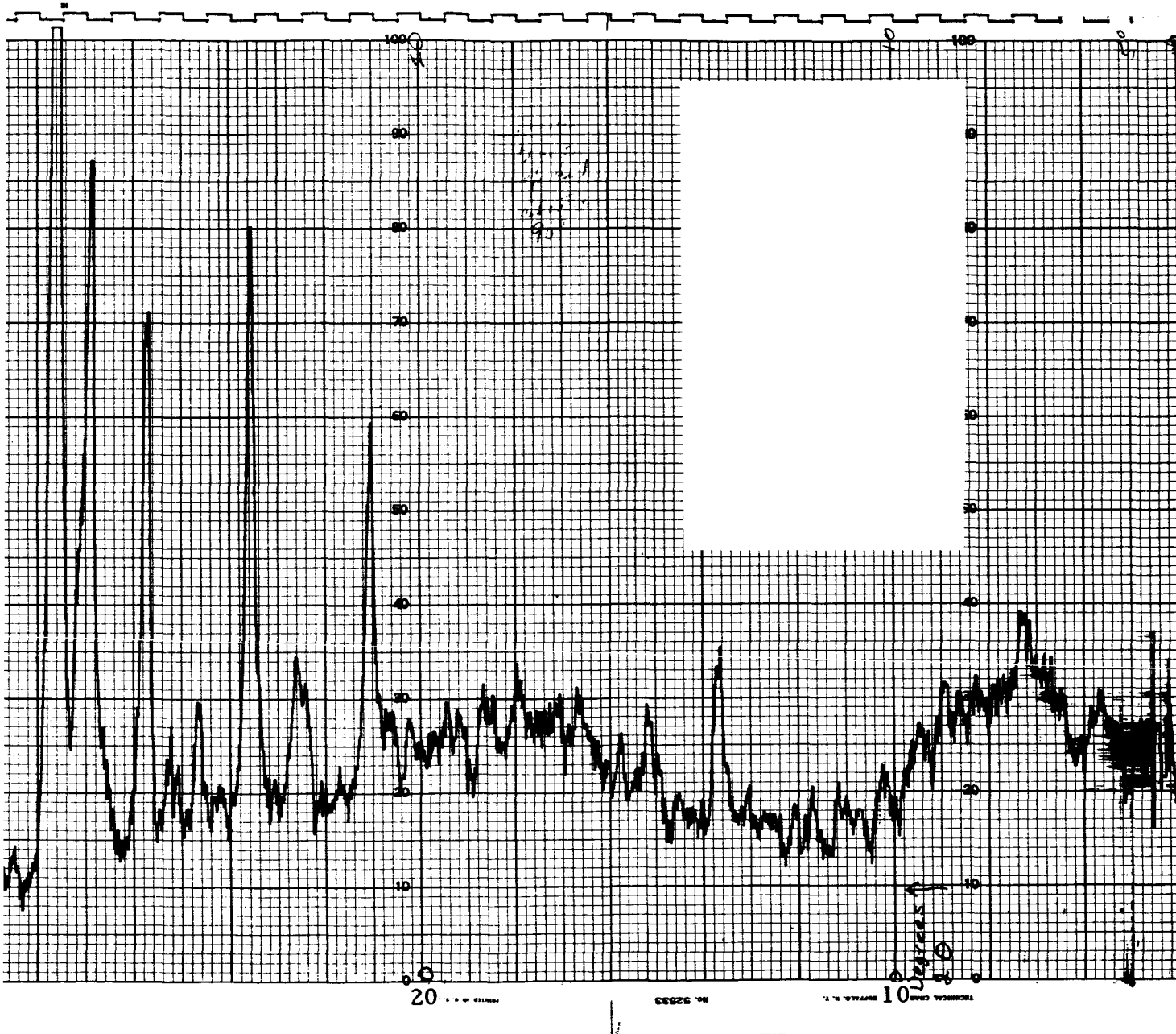


Figure 2-2 X-Ray Diffraction Peaks of the NH₄ Feldspar Made from the Madagascar Fe-Orthoclase

2.

The 1 gm of high purity ammoniated feldspar together with the previously synthesized 72-gm lot of somewhat less pure ammonium feldspar will be shipped to NASA when requested to do so.

2.2 REACTOR IRRADIATION OF PLAGIOCLASE

The radioactivity of the stored tubes of exposed labradorite has decayed to a level where one ionization chamber reads less than 0.5 mr/hr and another reads 0.2 mr/hr. These samples will be shipped to Houston as soon as requested by NASA.

SECTION 3

X-RAY PHOTOGRAPHIC INVESTIGATION

3.1 REFINEMENT OF POWDER SPECIMENS

In preparing for the long term experiment, (under conditions of high vacuum and high and low temperature) standard X-ray photographs of all 14 samples had to be taken, using the Bendix vacuum camera.

Photographs obtained using the material of mesh size < 325 mesh were unsatisfactory for several specimens. This was due to the fact that, although samples were ground to a size usually proved to be satisfactory for powder photographs, the distribution of sizes was such that there was a large fraction of crystallites with sizes only slightly less than 325 mesh. Since it would be extremely complicated to design a multiple specimen camera with the capability for specimen rotation, photographs of some samples were very spotty; that is, powder diffraction lines were very poorly defined. Thus, it was necessary, starting with the < 325 mesh samples, to continue grinding. Grain size was estimated to be at least 500 mesh on the average. This material was used for the final test specimens.

3.2 EVALUATION OF CAPILLARY TUBES

All samples were mounted in 0.2 mm diameter glass capillaries. Experiments with various-sized capillaries showed that absorption of the X-ray beam was excessive for larger samples. Yet it is necessary to place as much sample as possible in the beam path in order to obtain well defined powder lines without spots of high intensity from large single crystallites. The 0.2 mm size gave optimum conditions for all except the iron oxides, which are highly absorbing. Slightly smaller capillaries were thus chosen for the goethite and hematite.

3.3 BERYLLIUM WINDOW EFFECTS ON X-RAY FILM

It was found to be unnecessary to extend the X-ray film into the "negative" theta region of the camera, for which it was designed, in order to

provide a reference point for the determination of theta values for diffraction lines. Slight imperfections in the brazing of the beryllium window caused standard reference marks to appear on the film, which are defined by the diffuse X-ray background on the film. These reference points have been accurately calibrated using standard materials and a template prepared for rapid measurement of d-values. However accurate d-values (e. g., values reported here) are obtained by careful measurement on individual films using a scale accurate to 0.05 mm.

As a result of the fact that the beryllium window extends over the X-ray beam exit port, a dark diffuse scattered X-ray line appears in the very low theta region of each film. Superimposed on this are some single-crystal diffraction spots of beryllium. This is caused by the X-ray beam passing through the exit collimator and being diffracted by the beryllium window to the film before entering the leaded glass exit tube. Since the beryllium has a finite thickness and a very low absorption coefficient, scattered radiation passes directly up through the beryllium between the bordering steel walls. Although this may be esthetically displeasing, the resulting background is not sufficient to interfere with interpretation of specimen scattered diffraction lines, although this is not obvious on the reproduced films.

3.4 STANDARD VACUUM CAMERA PHOTOGRAPHS (FIGURES 3-1 to 3-8)

The resulting patterns (d-values in Table 3-1) are all satisfactory with the following qualifications:

- (1) Because of the inability to rotate samples, a relatively large diameter X-ray beam collimator and large samples were required to obtain well defined diffraction lines. This has resulted in lines being relatively broad. This effect has undoubtedly been augmented by line broadening as a function of small particle size. The results are entirely satisfactory and well within the predicted limits of broadening, however.
- (2) A very few samples, despite the care taken in obtaining minimal grain size, produced some spotty character of the lines. This is particularly true of actinolite where the spots can be attributed to the excellent prismatic cleavages resulting in elongated crystallites, and partially to the preferred orientation of the crystallites. All photographs are readily interpretable, however.

Standard Vacuum Camera Photographs

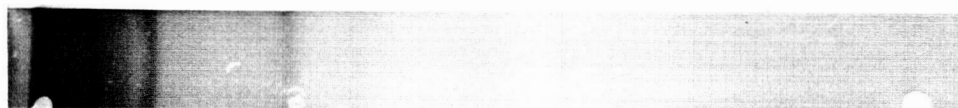


Figure 3-1 Antigorite - Mag-2x



Figure 3-2 Ca-Montmorillonite



Figure 3-3 Calcite - Mag-2x

Standard Vacuum Camera Photographs

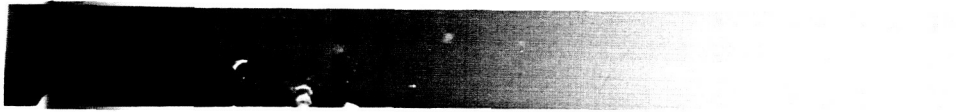


Figure 3-4 Goethite - Mag-2x



Figure 3-5 Hematite - Mag-2x

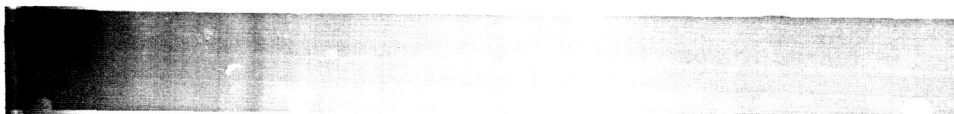


Figure 3-6 Muscovite - Mag-2x

Standard Vacuum Camera Photographs



Figure 3-7 Selenite - Mag-2x



Figure 3-8 Talc - Mag-2x

TABLE 3-1

D-VALUES OF POWDER SPECIMENS, A⁰

Bendix Vacuum Camera Patterns		Debye-Scherrer Camera Patterns		Bendix Vacuum Camera Patterns		Debye-Scherrer Camera Patterns	
d _{obs}	$\frac{I}{I_0}$	d _{obs}	$\frac{I}{I_0}$	d _{obs}	$\frac{I}{I_0}$	d _{obs}	$\frac{I}{I_0}$
Actinolite CuK _α				Gypsum CuK _α			
4.4	5	4.5	40	4.1	100	4.3	100
3.2	50	3.23	80	3.5	5	3.75	15
2.7	50	2.70	60	3.2	5	3.01	2
2.5	100	2.52	100	2.8	70	2.75	7
2.4	100	2.32	90	2.6	70	2.67	60
2.1	50	2.15	40	2.5	70	2.49	60
2.0	20	2.06	10	2.2	10	2.20	25
1.8	10	not on original list		2.0	15	2.08	50
1.7	10	1.67	30	1.9	15	1.87	50
1.5	10	1.50	30	1.8	40	1.80	80
1.4	10	1.36	20	1.7	30	1.77	70
Ammonium Feldspar CuK _α				1.6	30	1.66	70
4.2	20			Hematite MoK _α			
3.8	30			1.8	75	1.84	90
3.2	100			1.6	75	1.59	90
2.9	20	Material had not yet been synthesized when test minerals were		1.3	100	1.35	100
2.4	20	X-rayed during the previous		0.88	2	---	10
2.0	10	Reporting Period		Muscovite CuK _α			
1.8	10			4.3	70	4.5(pair)	100
1.7	10			3.8	20	3.85	30
Antigorite CuK _α				3.1	40	3.20	40
4.4	60	4.6	30	2.9	5	2.82	10
3.5	100	3.83	80	2.7	40	2.75	40
2.3	40	2.45	100	2.4	100	2.38	100
1.9	3	2.09	20	2.3	5	2.25	20
1.5	2	1.53	5	2.1	5	2.12	20
1.4	5	1.31	80	2.0	10	1.97	50
Basalt Glass CuK _α				1.8	5	1.70	40
The quantity of crystalline plagioclase in the sample was too small to cause observable diffraction lines on the standard vacuum camera photographs.		3.1	20	1.5	2	1.55	40
		2.5	100	1.4	30	1.35	40
		2.3	20	Natrolite CuK _α			
Calcite CuK _α				3.9	50	4.1	70
3.7	5	3.8	25	3.7	50	3.55	70
3.2	40	3.3	25	3.1	20	3.20	20
2.8	100	3.0	100	2.8	90	2.85	80
2.3	20	2.28	50	2.6	100	2.57	100
2.1	30	2.08	50	2.1	20	2.19	20
1.9	30	1.90	50	1.9	30	1.91	40
1.7	30	1.60	90	1.8	10	1.80	30
1.5	10	1.52	50	1.6	30	1.57	20
1.4	10	1.41	50	1.4	10	1.42	10
Ca-Montmorillonite CuK _α				1.37	5	1.38	10
4.2	100	4.5	100	1.3	5	1.31	10
3.8	100	4.05	50	Plagioclase CuK _α			
2.9	50	3.10	25	4.1	10	4.0	20
2.3	75	2.55	70	3.1	100	3.2	100
1.5	30	1.69	20	2.4	20	2.50	10
1.4	50	1.49	30	2.0	5	2.00	2
Goethite MoK _α				1.7	2	1.60	2
1.7	75	1.72	40	Talc CuK _α			
1.5	100	1.51	50	4.4	30	4.7	20
				2.9	60	3.1	50
				2.5	20	2.45	50
				2.3	100	2.20	100
				2.1	20	2.08	30
				1.9	10	1.85	30
				1.7	2	1.72	10
				1.5	10	1.52	20
				1.4	50	1.39	50
				Tektite CuK _α			
				No lines were observed, which is consistent with the non-crystalline nature of the material.			

- (3) Because of the iron content of the hematite and goethite samples, copper radiation is unsatisfactory for producing good patterns. In addition iron on longer wavelength radiation is highly absorbed. Therefore, these photographs were obtained using molybdenum radiation which results in a minimum number of lines being observable in the low theta region. The phases are still well defined, however.

3.5 COMPARISON OF D-VALUES

The resulting d-values obtained by careful measurement of the calibrated films are reproduced, with relative intensity data in Table 3-1, along with corresponding data obtained from standard Debye-Scherrer photographs of the same materials as presented in the preceding quarterly report. Not all lines of the Debye-Scherrer patterns are listed since many lines on patterns of some phases are too weak to be observed. The excellent correlation of values is obvious on examination of the table. Since even minor changes between photographs can be observed on direct visual comparison with the prepared standards, the resulting photographs should be very adequate to determine the occurrence of changes in the specimens in the long-term experiment.

SECTION 4

LONG-TERM EXPERIMENT

As explained in Section 5.2, the decision was made to run the long-term experiment in two totally separate vacuum chambers. The original cross-chamber with the 50 liter/sec ion pump would be used to test and X-ray the 14 mineral specimens of milligram weight, and a larger vacuum chamber (2-ft diam and 5-ft length) with a 500 liter/sec ion pump would be used to store and test the 14 mineral specimens, each weighing 5 grams, that will undergo chemical analysis at the end of the long-term experiment.

4.1 CROSS-CHAMBER WITH X-RAY SAMPLES

Preliminary tests were run with 6 samples (NH_4 feldspar, antigorite, Ca-montmorillonite, goethite, gypsum, and natrolite) to determine whether the combined gas load would be too much for the ion and sublimation pumps to handle. The powdered specimens were loaded into capillary tubes and each tube placed within a heater coil. The system was evacuated, and when the pressure reached the 1×10^{-8} torr range, the current was put into the heaters. The almost explosive volatilization of gases from the specimens swamped the pumps, and, almost instantly, the pressure rose to the 1×10^{-3} torr range. The electrical arrangement then experienced a corona discharge and arc to ground, which completely destroyed the heater filament and thermocouple connections (Figure 4.1).

These results indicated that gas loads generated at high temperatures and extremely high vacuum were too large for the ion and sublimation pumps to handle. Since the roughing pump has a greater capacity, it was decided to extend the roughing stage until the gas load had been reduced to a level where the ion pump could safely take hold and maintain the vacuum.

The capillary tubes were again filled with powdered minerals, and then installed in the test apparatus. The system was evacuated, while the specimens were cooled with LN_2 . The pressure gradually decreased to 9×10^{-9} torr but in a most peculiar manner. Instead of a uniform drop in pressure, the pumpdown rate was very erratic. It appeared that as the

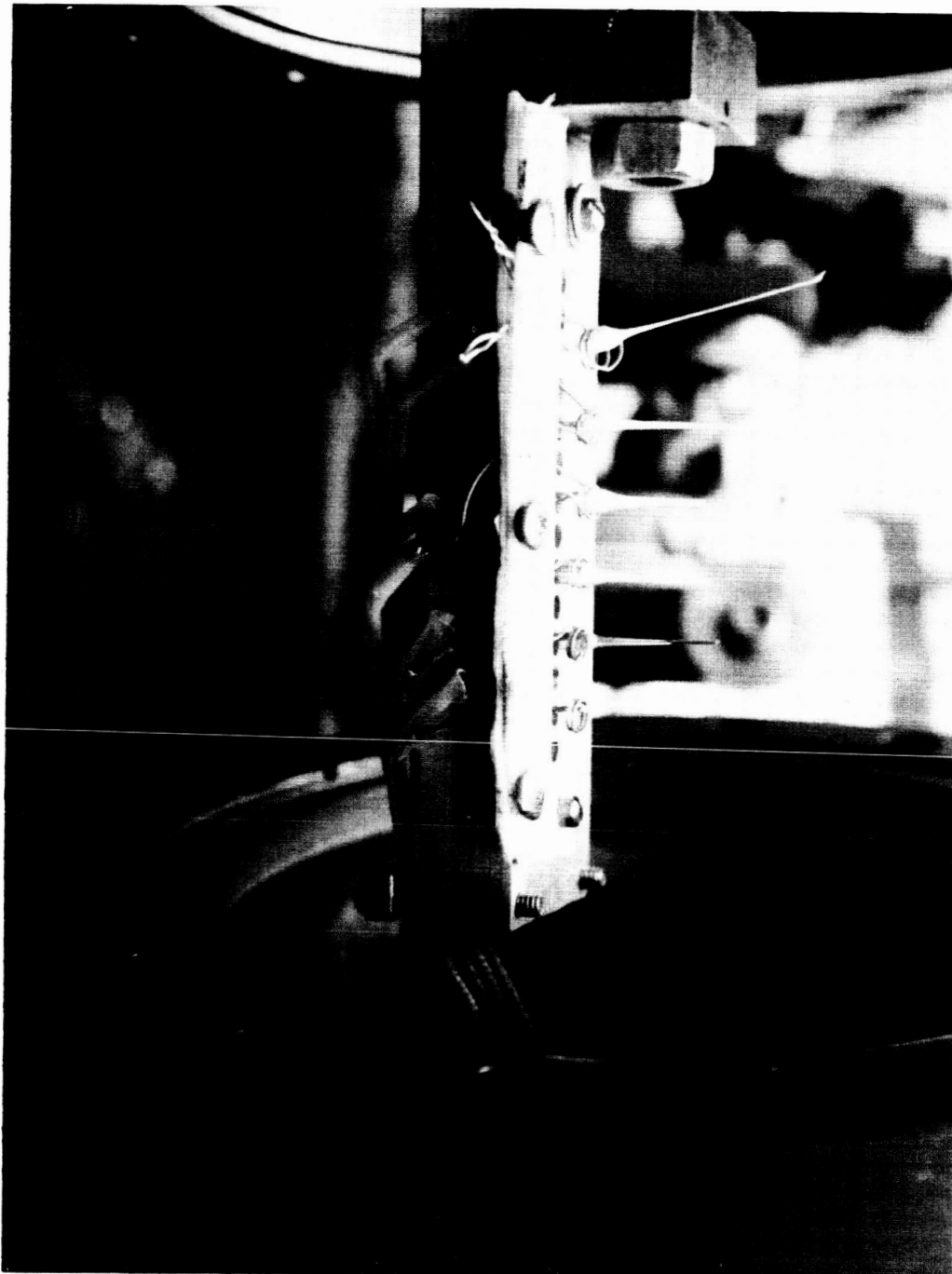


Figure 4-1 X-Ray Sample Holder Showing Burned Out Heater
Filament and Thermocouple Connections

pressure level dropped, transformation would occur in different minerals producing new volatiles. Once these gases had been evacuated, pumpdown would progress at a faster rate until another plateau was reached. The pressure would stabilize for a given length of time, and then the pattern would repeat itself. The commencement of the heating cycle produced a sudden rise in pressure to the 1×10^{-6} torr range.

Having gained invaluable experience from the preliminary testing described above, we were ready to proceed into the actual long-term experiment with considerably more confidence than we had at the beginning of the investigation. The 14 minerals have now been installed in the X-ray sample holder, the system has been sealed, pumpdown has commenced, and the long-term experiment is finally under way.

4.2 LARGE CHAMBER WITH CHEMICAL SAMPLES

Whereas the cross-chamber is situated in the X-ray Laboratory of the Department of Geology and Mineralogy, The University of Michigan, the second vacuum system has been set up in the laboratory at Plant II of Bendix Systems Division. A liquid nitrogen line connects this vacuum chamber directly to a 2800-gal LN_2 storage tank through an automatic filling controller (Figure 4.2). Another LN_2 control unit was affixed to our vacuum installation at The University of Michigan (Figure 4.3). These units permit the cooling operation to take place unattended.

Fourteen Erlenmeyer flasks, containing the chemical samples, have been emplaced inside the vacuum chamber on a stainless steel plate, which can alternately be used as a cold wall and hot tray (Figure 4.4). This sample holder was designed so that the heating and cooling operations would be external to the vacuum system. It was accomplished by brazing pipe coil to the underside of the tray for the LN_2 and inserting heater wire inside the coil for heating the samples. The latter has the advantage in that the gas load will not be increased by the outgassing of the heater wire.

Temperature control is achieved by a manual Variac and instrumented with 3 recording thermocouples. These are situated on the heater wire, on the plate, and in one of the samples. (Goethite) and the temperatures are read on a millivolt potentiometer. In the cross-chamber, thermocouples are located on the block holding the capillary tubes.

The 14 test minerals have been loaded into the Erlenmeyer flasks and installed inside the large vacuum chamber. Commencement of the long-term experiment occurred simultaneously in both chambers, and the results will be presented in the final report.

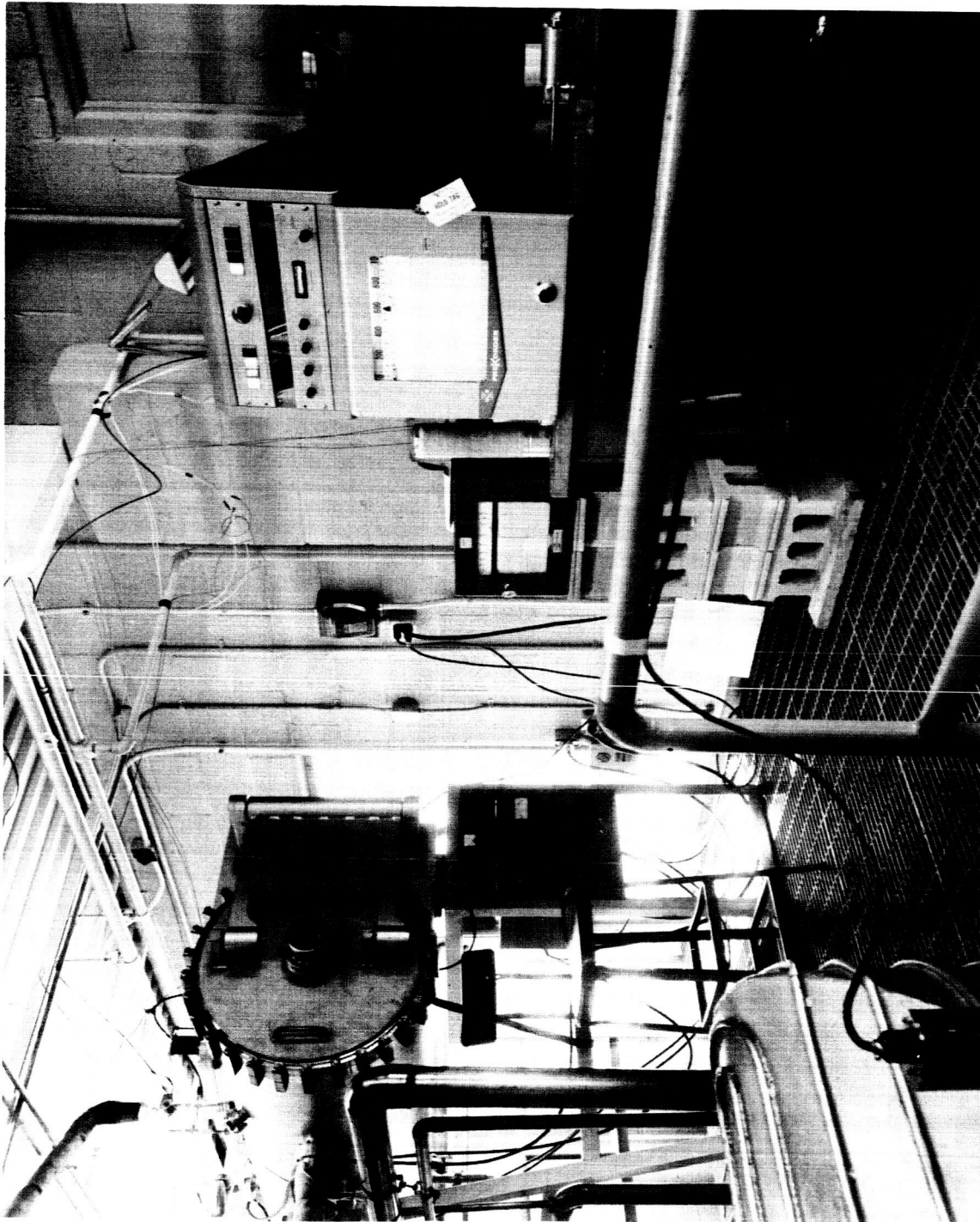


Figure 4-2 Large Vacuum Chamber with Control Units for Testing
Chemical Samples



Figure 4-3 Control Units for Cross-Chamber in The University of Michigan
Department of Geology and Mineralogy

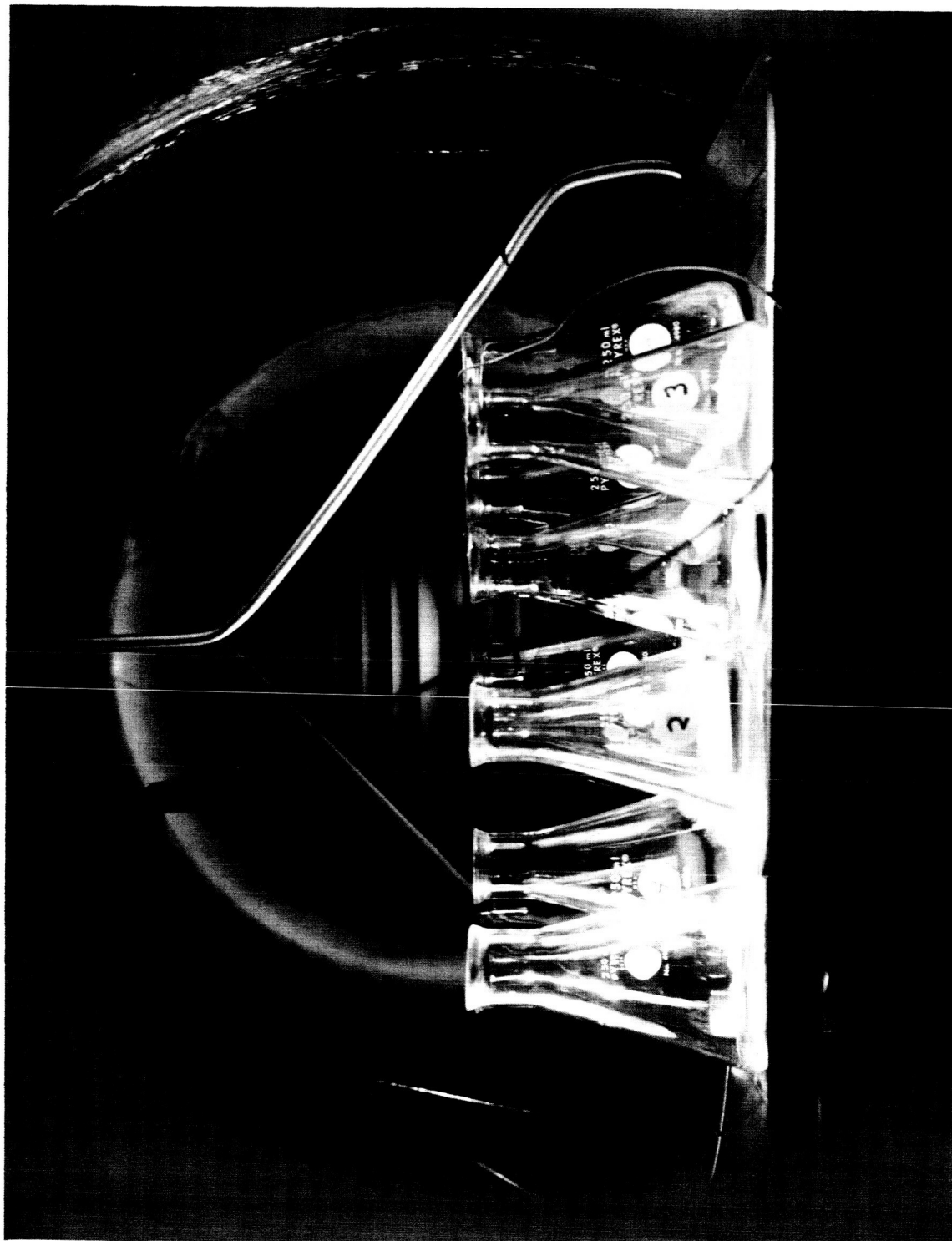


Figure 4-4 Sample Holder with 14 Erlenmeyer Flasks Inside the Large Vacuum Chamber

SECTION 5

FABRICATION OF LONG-TERM TEST APPARATUS

During this period the long-term test apparatus was assembled, checked out, and placed in operation. Leaks had been found and repaired and the ultimate vacuum capacity of 5.5×10^{-11} torr was finally achieved.

5.1 THE LEAKAGE PROBLEM

The ultrahigh vacuum required for the long-term experiment in combination with the relatively small pumping capacity (50 liters/sec) of the system can tolerate a leak rate on the order of 1×10^{-10} standard cc of helium/sec, which is near the detection limit of contemporary mass spectrometer gages. Leaks are particularly frustrating when the repair produces a new leak. This is actually what happened on the cold wall. After several leaks had been detected and repaired, a vacuum of only 1×10^{-9} torr could be achieved. A scan with the mass spectrometer revealed a leak in the weld between the shield and the reservoir. After repairing this defect, the cold wall was reassembled and installed in the test apparatus. Evacuation of the system disclosed no leaks, but with the sudden introduction of LN_2 the repair weld itself formed a new leak. Eventually the entire test apparatus was made leakproof.

5.2 THE PUMPDOWN PROBLEM

Upon checking out the multiple specimen vacuum camera containing the 14 capillary tubes loaded with the various test minerals, we quickly learned that the pumpdown rate reacted in a manner different from one of a homogeneous sample. Moreover, the extremely fine powders (< 325 mesh) tended to trap air molecules as well as volatile products, which, together, produced a fairly large gas load that effectively slowed down the evacuation process. It was also discovered that the sudden expansion of entrapped gases ejected the upper portion of the powdered specimen from the capillary tube. To study this phenomenon, a sample of Ca-montmorillonite was placed in a glass bell jar and subsequently evacuated. The powder was observed to "boil" and "fume" as the entrapped volatiles nucleated and rose to the surface. Here, eruptions scattered the ejected material onto the floor of the chamber.

The behavior of the powdered samples in vacuum provided cause for concern in being able to carry out the long-term experiment. It became apparent that should fuming occur in the capillary tubes, the level of powdered specimens might be lower than that of the X-ray beam, and thus, not available for taking photographs. There was also the likelihood of the gas load generated by the 70 grams of powder would completely swamp out the 50 liter/sec ion pump for an extended period of time. Surface eruptions on one or more samples could produce "cross-pollination," resulting in contamination of specimens. Finally, should the volume to area ratio of the test samples not be favorable low conductance from the interior would preclude attainment of internal equilibrium pressure.

These were the problems that had to be resolved before we could proceed with the long-term experiment. After some lengthy deliberations, it was decided that a second, larger vacuum chamber, equipped with a 500 liter/sec ion pump and likewise having an ultimate capacity of 5×10^{-11} torr, should be utilized for storing and testing the 70 grams of chemical samples, and that the original cross-chamber would be used for storing and testing the X-ray samples. Test procedures for the 2 chambers were synchronized so that both sets of specimens would experience equivalent temperature cycling.

This larger chamber has a working test space of 2-ft diameter by 5-ft length. Access is provided through a 2-ft diameter door opening at one end of the chamber. The chamber may be operated either in a horizontal or angular position up to 90° vertically. A specification sheet with a photograph of the chamber is attached (Figure 5.1).

Two ports and four feedthroughs are incorporated in the chamber. The 4-in. diameter pyrex observation ports can be replaced with quartz to permit solar simulation. One of the four feedthroughs is an eight-pin electrical connector. The other feedthroughs provide entries for liquid or gas, linear motion and rotary motion. If required, additional electrical feedthroughs may be substituted for the fluid and motion feedthroughs.

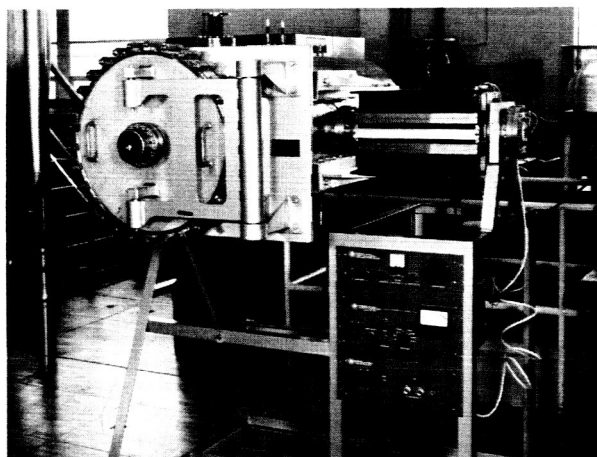
The chamber is rated to reach and maintain 5×10^{-11} torr. The pumping system incorporates a 500 liter/second ion pump, a 12000 liter/second titanium sublimation pump and a 5 cfm roughing system. Chamber performance is measured with a Redhead magnetron gauge.

date	specification number
Oct 64	1013 (Sheet 1 of 1)
department	
Environmental Laboratories	

specification sheet • developmental facilities

title
Extreme-High Vacuum Chamber

Mfr: Varian Associates



Solar simulation can be employed in this chamber by replacing the 4-in. Pyrex port with a quartz port. The fluid feedthru permits use of a thermal wall inside the chamber. The entire chamber can be rotated 90° to place the door at the top.

Size 2-ft diameter by 5 ft long (working space)

Range 5×10^{-11} torr

Pumps

Ion	500 liter/second
Titanium Sublimation	12,000 liter/second
Roughing	15 cfm

Access

- 1 end opening door, 2-ft diameter
- 1 Pyrex port, 4-in. diameter
- 1 8-pin feedthru
- 1 linear-motion feedthru
- 1 rotary-motion feedthru
- 1 fluid feedthru

Instrumentation Redhead magnetron gauge

General capable of 250° C bakeout
stainless steel inside finish

A separate investigation was initiated to determine the optimum roughing cycle that will minimize, if not eliminate, the boiling process. In conjunction with this study, a search for suitable sample containers was begun. The results of these experiments were subsequently incorporated in the the aforementioned procedures.

We found that a pumpdown rate from atmosphere to 500 microns in 16 hours prevented the powders from boiling in the capillary tubes. The ends of the capillary tubes were also plugged with fine fiberglass, and this provided a supplemental check against cross-pollination of specimens. Experiments with different types of sample containers indicated that when the sample was spread out in a thin layer, boiling did not take place. Consequently, we selected the 250 ml Erlenmeyer flask as the container in which to store the 5-gm sample. Since the cross-chamber is too small to accommodate 14 flasks, it served to further reinforce our decision that a larger vacuum chamber should be used for testing the chemical samples.

SECTION 6

PLANNED RESEARCH FOR THE FINAL QUARTER

The work to be carried out in the fourth quarter will follow closely that outlined in Bendix's Technical Proposal, BSD 965. The tasks to be performed in the last quarter are described below:

1. Complete the long-term experiment
2. Conduct chemical analysis of test samples stored in the large vacuum chamber.